# Temperature-dependent femtosecond-resolved hydration dynamics of water in aqueous guanidinium hydrochloride solution†

**Debapriya Banerjee, Pramod Kumar Verma and Samir Kumar Pal***

***Received 2nd April 2009, Accepted 13th July 2009***
***First published as an Advance Article on the web 31st July 2009***
**DOI: 10.1039/b906578d**

The influence of ion dissolution in water is still controversial. The challenge posed to the existing concept of dissolved ions acting as water structure makers and structure breakers through recent studies calls for more experimental evidence. The temperature-dependent relaxation dynamics of water in bulk and in ionic salt solutions can give an idea about the hydrogen-bonded network and hence the perturbation induced in the tetrahedral structure of bulk water subsequent to ion dissolution. In our study, the temperature dependence of the observed relaxation dynamics in bulk water and guanidinium hydrochloride reveals the activation energy needed to convert water from hydrogen bonded to the free forms and hence the difference in the hydrogen-bonded network in the close vicinity of the probe molecule. The results might prove helpful to understand the interaction of hydrophobic amino acid residues with guanidinium hydrochloride during protein denaturation.

## Introduction

The importance of water in the living world embraces fields as varied as biochemistry, synthetic chemistry, earth sciences and biology. The properties of water emanate from the unique hydrogen bonding network. This has triggered research on understanding the hydrogen bonding in water.[1–3] Experimental and theoretical techniques give the picture that the local structure of water, while certainly disordered, is more or less tetrahedral with approximately 3–5 hydrogen bonds per molecule.[4] A typical water molecule makes two hydrogen bonds through its hydrogen atoms and two hydrogen bonds through its oxygen atoms. The orientational dynamics of water in bulk have been studied by Bakker *et al.*[5] using femtosecond mid-infrared spectroscopy and the orientational diffusion time of bulk water is ~4 ps. Femtosecond resolved solvation studies by Maroncelli *et al.*[6] and Barbara *et al.*[7] reveal that the solvation response of bulk water is bimodal. There is a fast inertial response indicating librational motions and a slower diffusional motion. Water is a universal solvent dissolving a wide variety of ions (monoatomic or molecular), charged species and biomolecules. The dissolution of solutes in water is accompanied by the formation of hydration shell around the solute. The suggestion by Cox and Wolfenden,[8] that the structure and dynamics of hydrogen bonds in water might be perturbed on ion dissolution have initialized studies on the ion-induced modification of the tetrahedral structure of water.[3,9] It has been proposed that ions with high charge density (kosmotropes) and those with low charge density (chaotropes) affect the water structure differently[10] and the terms "structure makers" and "structure breakers" have been universally used to describe the perturbation of the aqueous environment.[11] In fact, earlier reports suggest that important biophysical processes, *e.g.* denaturation of proteins, is due to the water structure breaking property of the commercially used chaotropic denaturants urea and guanidinium hydrochloride.[9] However, the assignment of ions as structure makers or breakers was ambiguous and generated several controversies.[12]

A series of recent femtosecond mid infrared studies by Bakker *et al.*[5,13] showed that the addition of ions have no influence on the rotational dynamics of water beyond the first solvation shell, thus challenging the prevalent conception of ions being water structure makers and structure breakers. In a recent study by Mancinelli *et al.*,[3] combinations of neutron diffraction data and computer modeling have been used to show that the effect of the perturbation on the dissolution of ions extended to the second and third hydration shells.

It is to be noted that the hydrogen-bonded structure of the water leaves its imprint in the activation energy barrier needed to convert the water molecule from the hydrogen bonded to the free form. The corresponding activation energy can be estimated from their temperature-dependent relaxation dynamics,[14,15] which in turn can be indirectly estimated from their solvation response to an excited state dipole.[16] Temperature-dependent picosecond resolved solvation techniques have been used to estimate the activation energies of confined waters in nanopools[15,17,18] and at biointerfaces.[19] Although the energetics of the dynamically slower biological waters and nanoconfined waters have been experimentally determined through solvation techniques, the energetics of the faster bulk water has been established mainly through *ab initio* calculations.[20] Direct experimental evidence of the same is lacking in literature. The dynamics of the bulk waters fall in the femtosecond regime, and the potential stumbling block might be the unavailability of commercial temperature-dependent femtosecond upconversion setups for temperature-dependent studies. In the present study, we report the design of a temperature-dependent accessory

*Unit for Nano Science & Technology, Department of Chemical, Biological & Macromolecular Sciences, S. N. Bose National Centre for Basic Sciences, Block JD, Sector III, Salt Lake, Kolkata, 700 098, India. E-mail: skpal@bose.res.in; Fax: +91 33 2335 3477*

† Electronic supplementary information (ESI) available: Details of the construction of TRES and the design of the temperature-dependent accessory. See DOI: 10.1039/b906578d

compatible with commercially available femtosecond setup for temperature-dependent femtosecond studies. The hydrophobic fluorophore Coumarin 500 (C500) performs the dual role of a solvation reporter and a mimic for small moieties like amino acid residues. The temperature-dependent environmental dynamics in bulk water and in guanidinium hydrochloride solution, reported by the fluorescent probe have been exploited to estimate the corresponding activation energies. The activation energy reflects the energetic barrier needed to convert water from hydrogen bonded to the free forms and hence the hydrogen-bonded structure near the probe. The energetic barrier to rotational motion of the ions has also been estimated from the temperature-dependent rotational dynamics. Since both the rotational dynamics and the solvation response characterize the microenvironment of the probe, the results might shed light into the hydration structure and energetics of water in the immediate vicinity of an ion or charged chemical species. Since amino acids are small hydrophobic molecules like the probe used in our present study, the results might be useful to understand the dynamics of protein denaturation.

## Materials and methods

Guanidinium hydrochloride (GdmCl) is obtained from Sigma. The fluorescent probe Coumarin 500 (C500) is a product of Exciton. Millipore water having resistivity $18.2 \times 10^{-6}$ Ω cm is used as the water sample and to prepare aqueous GdmCl. The solutions of C500 are prepared by dissolution of the solid probe in the respective solvents and subsequent filtration to remove suspended particles in solution.

Steady-state absorption and emission are measured with Shimadzu UV-2450 spectrophotometer and Jobin Yvon Fluoromax-3 fluorimeter respectively, with a temperature controller attachment from Julabo (model: F32). The temperature-dependent femtosecond-resolved fluorescence is measured using a femtosecond upconversion setup (FOG 100, CDP) along with an indigenous temperature controller setup (see ESI†). The sample is excited at 410 nm (0.5 nJ per pulse), using the second harmonic of a mode-locked Ti-sapphire laser with an 80 MHz repetition rate (Tsunami, Spectra Physics), pumped by 10 W Millennia (Spectra Physics). The fundamental beam is frequency doubled in a nonlinear crystal (1 mm BBO, $\theta = 25°$, $\phi = 90°$). The fluorescence emitted from the sample is up-converted in a nonlinear crystal (0.5 mm BBO, $\theta = 10°$, $\phi = 90°$) using a gate pulse of the fundamental beam. The upconverted light is dispersed in a double monochromator and detected using photon counting electronics. A cross-correlation function obtained using the Raman scattering from water displayed a full width at half maximum (FWHM) of 165 fs. The viscosity measurements are done in a viscometer from Anton Paar (Austria; model: AMVn); the instrumental resolution for the measurement of viscosity is $1 \times 10^{-4}$ gm cm$^{-3}$.

The femtosecond fluorescence decays are fitted using a Gaussian shape for the exciting pulse. The details of the construction of time resolved emission spectra (TRES) can be found in the ESI.† The time-dependent fluorescence Stokes shifts, as estimated from TRES are used to construct the normalized spectral shift correlation function or the solvent correlation function, $C(t)$ defined as,

$$C(t) = \frac{(\nu(t) - \nu(\infty))}{(\nu(0) - \nu(\infty))} \quad (1)$$

where, $\nu(0)$, $\nu(t)$ and $\nu(\infty)$ are the emission maximum (in cm$^{-1}$) at time zero, $t$ and infinity. The $\nu(0)$ value was obtained from the processing of our experimental data as described in the ESI.† The $\nu(\infty)$ values had been taken to be the emission frequency beyond which an insignificant or no spectral shift is observed. The $C(t)$ represents the temporal response of the solvent relaxation process, as occurs around the probe subsequent to its photoexcitation and the associated change in the dipole moment. For anisotropy ($r(t)$) measurements, emission polarization is adjusted to be parallel or perpendicular to that of the excitation and anisotropy is defined as,

$$r(t) = \frac{[I_{para}(t) - I_{perp}(t)]}{[I_{para}(t) + 2 \times I_{perp}(t)]} \quad (2)$$

where $I_{para}$ and $I_{perp}$ are emission intensities with the emission polarizer adjusted parallel and perpendicular to that of excitation.

## Results and discussion

Fig. 1a shows the absorption and emission spectra of Coumarin 500 (C500) in water. The temperature-dependent absorption and emission of the probe in water does not show appreciable shifts in the positions of the corresponding absorption and emission maxima, suggesting that C500 retains its structure and optical properties in the temperature range studied. The absorption and the emission spectra of the probe in 6 M guanidinium hydrochloride (GdmCl) solutions (Fig. 1b) also does not show any shift in the position of absorption or emission maxima, compared to that in water. It has been reported that the addition of salt causes a red shift in the steady state absorption and emission spectra of the probe solute compared to that in pure solvent.[21] The magnitude of such shifts decreases when the solvent polarities increase and are unobservable for water and formaldehyde systems. However, there is a significant increase in the solubility of C500 in 6M GdmCl. The increased solubility of C500 in GdmCl parallels that of amino acids.[22] The increased solubility of both C500 and amino acids in GdmCl might be indicative of the similarity in the mode of interaction of the amino acids and the hydrophobic probe C500. Thus, it is tempting to exploit the fluorescence solvochromism of the probe to compare the microenvironments of the probe in water and in the chaotropic GdmCl. Since GdmCl initiates protein denaturation,[23,24] the results might be relevant to understand the fundamental process of protein denaturation.

To answer the fundamental question of how the dynamics of water in the immediate vicinity of a charged species (here GdmCl) differ from those of pure water, we monitored the dynamics of environmental relaxation, using the temporal evolution of the fluorescent Stokes shift technique.[25] Fig. 2a shows the representative fluorescence transients at the blue and red ends of the emission spectrum at 10 °C in bulk water. The fluorescence transient at the blue end shows fast decays of ~200 fs and 1 ps, which are converted to corresponding rises in the red end, indicating solvation stabilization. The solvation stabilization is associated with a spectral shift of 1121 cm$^{-1}$ in 8 ps window, as borne out by the time resolved emission spectra (TRES, inset of Fig. 2a). The temporal decay of the solvation correlation function, $C(t)$ is

 

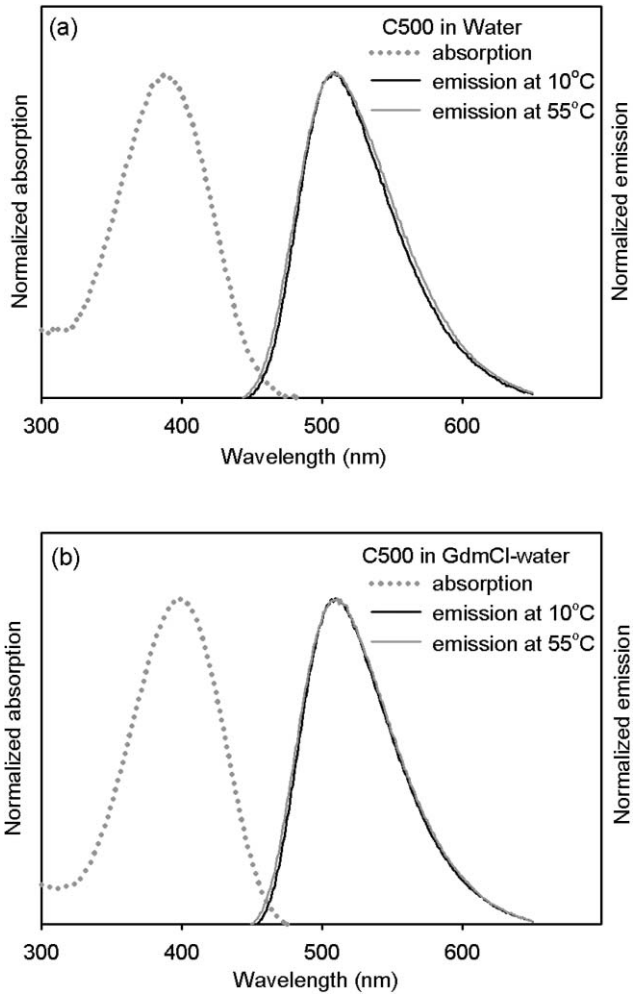


**Fig. 1** The absorption and emission spectra of Coumarin 500 in water (a) and 6M guanidinium hydrochloride (GdmCl) (b).

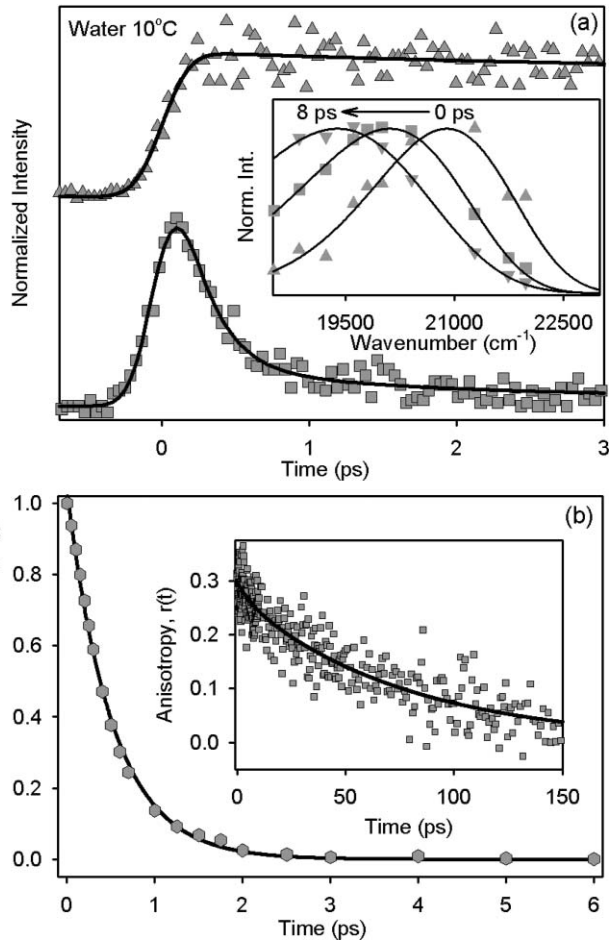


**Fig. 2** The fluorescence transients at the blue and red ends of the emission spectrum (a), the TRES (a, inset), the temporal decay of the solvent correlation function (b) and rotational anisotropy (b, inset) in water at 10 °C.

biexponential having time constants of ~300 fs and 1 ps (Fig. 2b). The dynamics of bulk water, studied by Maroncelli *et al.*,[6] reveals a bimodal nature of the solvation response. The solvation response is fitted with a Gaussian component of <50 fs, representing the fast solvent inertial motions and a longer component characterizing the diffusional motion of water. Barbara *et al.*[7] also obtained a bimodal distribution yielding time constants of 0.16 ps (33%) and 1.2 ps (67%). Fig. 3a depicts representative fluorescence transients taken at the extreme ends of the emission spectrum of C500 in 6M GdmCl at 10 °C. The decay of the fluorescence transient at the blue end of the emission spectrum is fitted with time constants of ~400 fs and 3 ps, which are slower than that in water. Corresponding rises are seen in the red end. The TRES (inset of Fig. 3a) reveal a spectral shift of 950 $cm^{-1}$ in 10 ps window. The $C(t)$ decay (Fig. 3b) in GdmCl is bimodal yielding time constants of 500 fs and 2.3 ps, reflecting slower environmental dynamics compared to the bulk solvent. To determine the extent of solvation dynamics captured through our instrumental resolution, we have determined the loss in the dynamic Stokes shift using the procedure developed by Fee and Maroncelli,[6] where $\nu^{p}_{em}(0)$ can be calculated by the following equation:

$$\nu^{p}_{em}(0) = {}^{p}_{abs} - [\nu^{np}_{abs} - \nu^{np}_{em}] \quad (3)$$

where $\nu^{p}_{abs}$, $\nu^{np}_{abs}$, and $\nu^{np}_{em}$ are the absorption peak in polar solvent, absorption peak in nonpolar solvent, and emission peak in nonpolar solvent, respectively. In the present study, we use cyclohexane as the nonpolar solvent with absorption and emission maxima of C500 at 360 and 410 nm, respectively. Water is used as the polar solvent in which the C500 produces an absorption peak at 390 nm. We calculated a ~28% loss in the dynamical Stokes shift. This loss finds its origin in the initial ultrafast decay of timescale faster than 50 fs.[6]

The slower dynamics in GdmCl might be indicative of ion–probe interaction, as discussed below. It is to be noted that when ions (monoatomic or molecular) or charged species of macromolecules are dissolved in water, a hydration shell is formed around the dissolved solute. The nature of the hydration shell is governed by the interactions between the water molecules and the charged solute (here GdmCl).[26,27] The water molecules near the GdmCl are different from those of bulk water and are bound-type biological water molecules.[28] The dissolution of ions is likely to reflect itself in the solvation response of the solvent and this has triggered the studies on the effect of ion dissolution on the observed environmental dynamics.[21,29] These studies reveal that the ion dissolution primarily affects the longer part of the solvent response.[29] The dynamics in ionic solutions are comparably

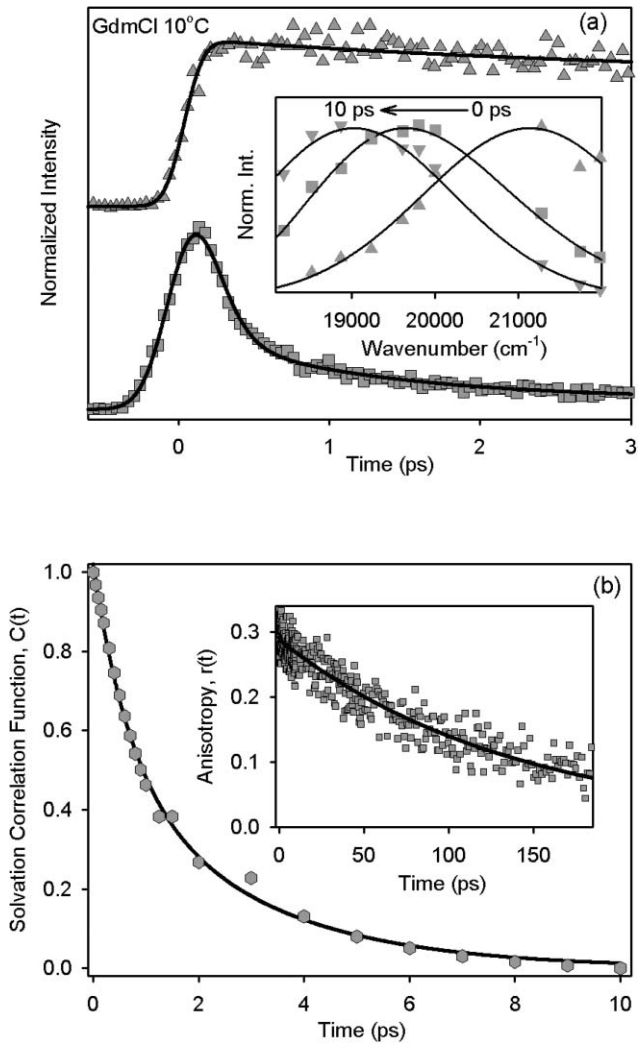


**Fig. 3** The fluorescence transients at the blue and red ends of the emission spectrum (a), the TRES (a, inset), the temporal decay of the solvation correlation function (b) and rotational anisotropy (b, inset) in 6 M guanidinium hydrochloride at 10 °C.

slower than that in the pure solvent[21] and decrease rapidly with increasing concentration of the added salt.[30] Maroncelli *et al.*[21] have studied the effect of ion dissolution in various solvents on the dynamics of environmental relaxation. They have modeled their observations in the light of interactions between the ion and the probe molecule and rationalized the longer nanosecond dynamics in ionic solutions as an activated process, representing the replacement of water molecules by solute in the solvation shell of the probe anion. The slower solvation dynamics in 6 M GdmCl solutions have also been reported for tryptophan solvation by Zewail group.[31] The slower environmental dynamics might be indicative of C500–GdmCl interaction.

The probe–GdmCl interaction, if any would likely alter the probe environment, as shown in Scheme 1. It is therefore, essential to identify the microenvironment in which the probe resides. In this regard, we measure the temporal anisotropy decay, $r(t)$ of C500 in water and in 6 M GdmCl solutions. The decay of fluorescence anisotropy of the probe in water at 10 °C is shown in the inset of Fig. 2b. The probe in water at 10 °C exhibits a single rotational mode with a time constant of 66 ps. The time constants agree well with the rotational motion of similar sized bodies in water. At 10 °C, the rotational motion of C500 ($\tau_r = 158$ ps, inset of Fig. 3b) in 6 M GdmCl is slower than that in water (Table 1). Viscometric studies reveal the bulk viscosity of 6 M GdmCl at 10 °C to be 2.1 cP, compared to the bulk viscosity of 1.30 cP in water at 10 °C.[32] It is interesting to observe that at 10 °C, the bulk viscosity increases by a factor of 1.6 in GdmCl solutions compared to that of water, however, the rotational correlation time of the probe shows a 2.4-fold increase. The rotational relaxation time, $\tau_r$ of the probe

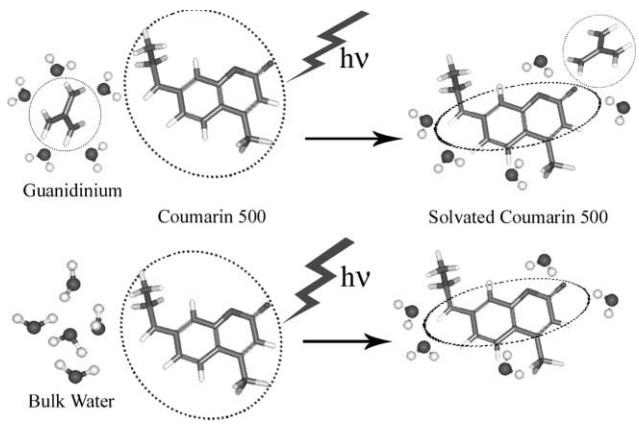


**Scheme 1** Model of the interaction between C500 and the solvent environment, showing the interfacial dynamics studied through the excitation of C500 and the response of the environment. The excited state dipole moment, created in the C500 molecule by femtosecond pulse creates an instantaneous field around the molecule. The ordered water molecules around the ion in ground state of C500 along with the ion start to respond to the instantaneously created field. Due to the response of the bound water molecules and the ion, the solvation gets slower compared to the bulk water solvation represented at the lower panel.

**Table 1** Temperature-dependent viscosities and rotational relaxation time constants of coumarin 500 in water and 6 M guanidinium hydrochloride (GdmCl)

| | | | | Simple SED ($f = 1$) | Modified SED ($f = 1.15$) | |
|---|---|---|---|---|---|---|
| $T$/°C | $\tau_{rot}$ (GdmCl)/ps | $\tau_{rot}$ (water)/ps | Bulk-viscosity of 6 M GdmCl/cP | Micro-viscosity of 6 M GdmCl ($C = 1.0$)/cP | Micro-viscosity of 6 M GdmCl ($C = 1.0$)/cP | Micro-viscosity of 6 M GdmCl ($C = 0.664$)/cP |
| 4 | 204 | 75 | 2.4 | 3.9 | 3.4 | 5.1 |
| 10 | 158 | 66 | 2.1 | 3.1 | 2.7 | 4.0 |
| 20 | 134 | 52 | 1.7 | 2.7 | 2.4 | 3.5 |
| 34 | 105 | 43 | 1.3 | 2.2 | 2.0 | 2.9 |
| 55 | 88 | 35 | 1.0 | 2.0 | 1.8 | 2.5 |

 

is related to the local microviscosity $\eta_m$ of the probe environment through the modified Stokes–Einstein–Debye equation (SED),[33,34]

$$\tau_r = \frac{\eta_m V_h}{k_B T} \quad (4)$$

where $k_B$ is the Boltzmann constant and $T$ is the absolute temperature. $V_h$ is the hydrodynamic volume of the probe and given by the expression:

$$V_h = V_m f C \quad (5)$$

where $f$ is the shape factor ($f = 1$ for a spherical probe) and $C$ represents solute–solvent coupling constant ($C = 1$ for "stick" condition and $C < 1$ for the "slip" condition) and $V_m$ is the molecular volume of the probe.[35] In case of both parameters $f$ and $C$ being equal to 1, then the equation reduces to the original simple SED equation,

$$\tau_r = \frac{\eta_m V}{k_B T} \quad (6)$$

In order to estimate microvisocities we have used the simple SED (eqn (6)) as well as the modified SED (eqn (4) and (5)) model considering realistic $f$ and $C$ values as follows. The probe C500 is assumed to be an oblate ellipsoid having molecular volume of ~198 Å$^3$ (Scheme S2, ESI†). For an oblate ellipsoid,[33,34] the value of $f$ is calculated using the equation,

$$f = \frac{2(p^4 - 1)}{3[(p^2 - 1)p^2(p^2 - 1)^{-1/2}\arctan(p^2 - 1)^{1/2} + p^2]} \quad (7)$$

where $p$ is the axial ratio (ratio of major axis to the minor axis) of the ellipsoid. In the case of C500, the shape factor, $f$, is estimated to be 1.15. As the coupling constant $C$ also depends on the boundary condition (slip or stick), we have estimated the microviscosities by considering the coupling factor to be less than unity (0.664) for slipping boundary condition as calculated for a nonspherical probe.[36] The estimated microviscosity values are tabulated in Table 1 and plotted in Fig. 4a for the visual representation. It is clear from Table 1 and Fig. 4a that the microviscosity of the probe C500 in close association with GdmCl at various temperatures are higher than those of the bulk viscosities. Microviscosity is the friction experienced by a probe molecule at the microscopic scale; it is an important parameter for characterizing the local environment because modest changes in local viscosity lead to variation in physical as well as chemical properties. The difference in bulk viscosity of the solution and the microviscosity experienced

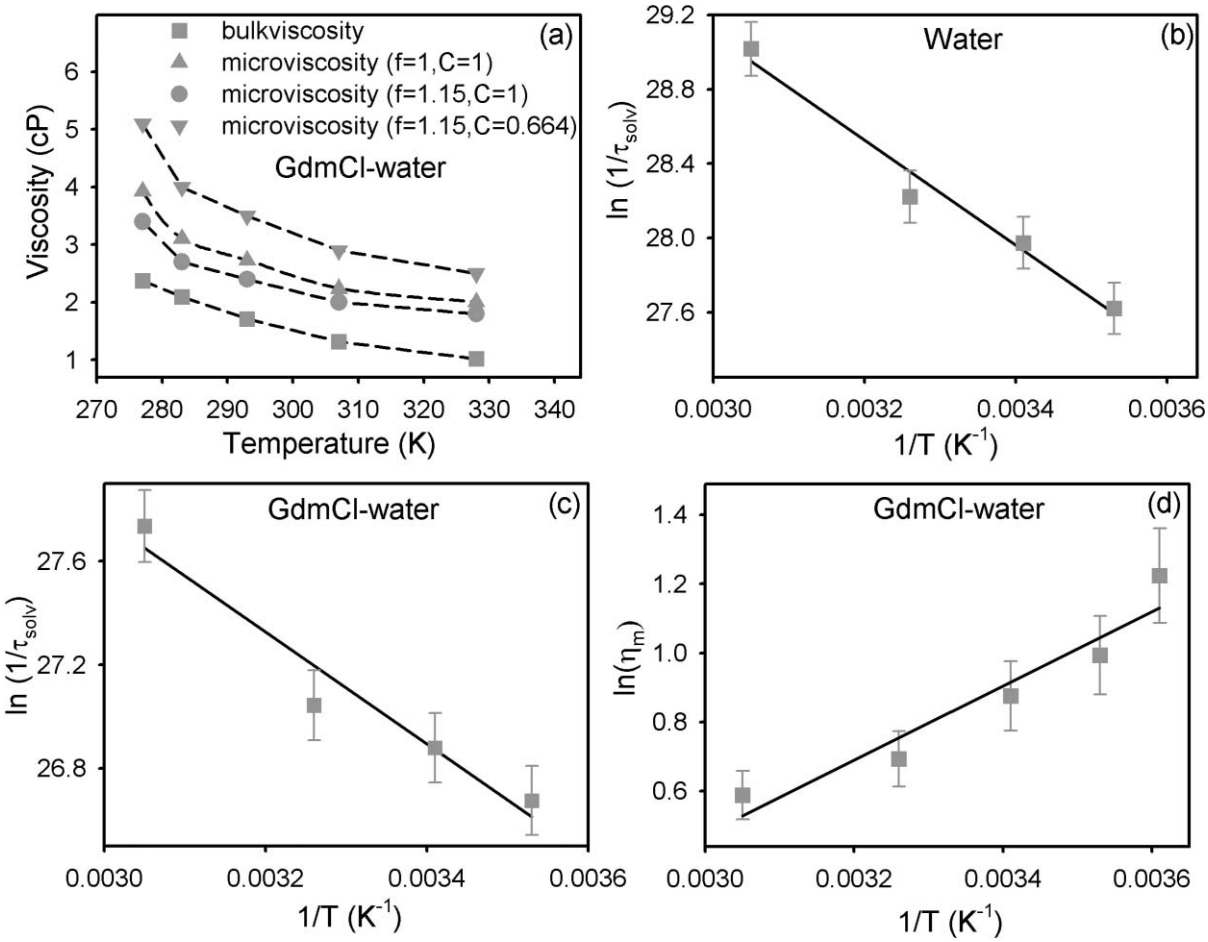


**Fig. 4** (a) The plots of bulkviscosity ($\eta$) and microviscosities ($\eta_m$) *vs.* temperature ($T$) for guanidinium hydrochloride. The broken lines are guide to eye. (b and c) The plots of $1/\tau_{solv}$, against $1/T$ for water and guanidinium hydrochloride solutions. The solid line is the corresponding numerical fit of the Arrhenius equation. (d) The plot of ln $\eta_m$ against $1/T$ for 6 M guanidinium hydrochloride solution. The solid line is the corresponding numerical fit of Arrhenius type plot.

by the probe clearly indicates that the probe is located in a region of greater microviscosity. Using femtosecond mid-infrared spectroscopy, Bakker *et al.* have shown that the viscosity in the solvation shell of ions is much greater than that of bulk.[13] The greater microviscoity experienced by C500 might thus be indicative of its location in the close proximity of the GdmCl ions, probably in its solvation shell, indicating ion-probe association. Such interaction of the hydrophobic probe with GdmCl might have its origin in preferential hydrophobic interactions. This preferential interaction of small hydrophobic moieties with guanidinium cation, resulting in their higher solubility compared to that in water is reported in literature.[22] Indeed, the interaction of hydrophobic amino acid residues with denaturants like GdmCl is currently thought of as initialization of the protein denaturation process,[10] contrary to the previous theory of the alteration of water structure by the chaotropic denaturants like urea and guanidinium hydrochloride.[9] The location of the probe in the solvation shell of the GdmCl cation might provide a rationale for the slower solvation response in GdmCl as discussed earlier. The slower solvation in GdmCl solutions can be thought of due to the slower orientational motion of the water molecules in the hydration shell of the guanidinium cation.[37]

The higher microviscosity compared to that in water indicated from the slower rotational motions of the probe in GdmCl, coupled with the slower solvation response provides clear indication of the location of C500 in the solvation shell of the guanidinium cation. In this regard, we independently monitor the temperature-dependent rotational dynamics of the probe and the relaxation dynamics of its environment in bulk water and in GdmCl. The temperature-dependent time constants of the environmental dynamics in bulk water and in 6M GdmCl have been tabulated in Table 2. At each temperature the response is bimodal, the magnitude of the faster component remains practically constant, and the slower component becomes progressively faster with increasing temperature for both the systems. Since the longer time constant represents the diffusional motion of the solvent molecules,[6] the temperature dependence of this rate would give an idea about the activation energy for the conversion of hydrogen-bonded solvent to the free forms according to the following relation,[28,38]

$$k_{\mathrm{bf}} \approx \frac{1}{\langle \tau_{\mathrm{solv}} \rangle} = \left(\frac{k_{\mathrm{B}}T}{h}\right)\exp\left(\frac{-\Delta G}{RT}\right) \tag{8}$$

here, $\tau_{\mathrm{solv}}$ represents the slower dynamics, $k_{\mathrm{bf}}$ is the rate of bound-to-free conversion, $h$ is the Planck's constant and $\Delta G$ is the corresponding activation energy. The temperature dependence of the solvation time scales can be exploited to obtain the activation energies of the solvating moieties through the Arrhenius equation.[28,38–40] Fig. 4b and 4c show the Arrhenius plots for water and GdmCl solutions. The activation energy corresponding to bulk water is estimated to be ~5.5 kcal mol$^{-1}$ and is consistent with the values estimated from *ab initio* studies.[20,41] The activation energy in 6M GdmCl is found to be ~3.6 kcal mol$^{-1}$. This activation energy value (3.6 kcal mol$^{-1}$) is of the order of 2.4–4 kcal mol$^{-1}$, the energy barrier calculated for the transition from the bound-type water to free-type water (hydrogen bonded to polar head group of reverse micelle and micellar surface[17,18]). Since the sparingly soluble C500 nests in the hydration shell of GdmCl, these activated processes represent the dynamic interconversion between free and bound waters in the solvation shell of the Gdm cation. The solvation structure of the guanidinium ions reveals a few water molecules bound through weak hydrogen bonds in the plane of the cation.[37] The presence of such loosely bound water in the environment of C500 characteristic of the water molecules associated with the solvation of Gdm cation, confirm close association of C500 with the latter.

**Table 2** Temperature-dependent solvation correlation functions, $C(t)$ in water and 6 M guanidinium hydrochloride (GdmCl)

| | $C(t)$, water/ps | | $C(t)$, GdmCl/ps | |
|---|---|---|---|---|
| $T$/°C | $\tau_1$ | $\tau_2$ | $\tau_1$ | $\tau_2$ |
| 10 | 0.31 | 1.01 | 0.51 | 2.32 |
| 20 | 0.33 | 0.71 | 0.56 | 2.12 |
| 34 | 0.38 | 0.55 | 0.54 | 1.92 |
| 55 | 0.30 | — | 0.8 | — |

A parallel understanding of the microenvironment around C500 can be carried out by following the temperature dependence of the rotational relaxation times. Table 1 lists the rotational relaxation times of C500 of water and 6M GdmCl at different temperatures. As observed from the table, $\tau_{\mathrm{r}}$ becomes faster upon increasing the temperature. It is evident from the Fig. 4a and Table 1 that the microviscosities are always higher than the bulk viscosity at all temperatures irrespective of use of the modified SED or simple SED, revealing the fact that the hydration structure near the probe and hence GdmCl is different from that of bulk water. It is observed that both $\eta$ and $\eta_{\mathrm{m}}$ decreases gradually with increasing temperature indicating that the probe experiences less rotational hindrance at higher temperature. The ease of rotation at different temperatures is an activated process and can be related to the compressibility of the probe environment. It has been shown earlier that the compressibility of loosely bound waters at the reverse micellar surface, energetically similar to those around Gdm cation, increases with increasing temperatures.[14] The microviscosity changes with temperature following the relation,[42]

$$\eta_{\mathrm{m}} = \eta_0 \exp\left(\frac{-E^*}{RT}\right) \tag{9}$$

where $E^*$ means activation energy for the viscous flow. The plot of $\ln \eta_{\mathrm{m}}$ (obtained using modified SED with $f = 1.15$ and $C = 1$) against $1/T$ (Fig. 4d) can be linearly fitted within the experimental error of ±10%. In the case of aqueous micellar solution the deviation of linear behavior of the experimental data of temperature-dependent microviscosity has also been explained in presence of higher order aggregates in the solution in the close proximity of Kraft temperature.[42] In our case the nonlinearity is within 10% experimental error and might also be due to some association of the ion with probe C500. The $E^*$ value is estimated to be 2.1 kcal mol$^{-1}$. We have also calculated $E^*$ using eqn (9) for the other two cases, *i.e.* simple SED ($f = 1$, $C = 1$) and modified SED with slipping boundary condition ($f = 1.15$ and $C = 0.664$) and values calculated are found to be similar (2.3 kcal mol$^{-1}$). Note that these values are smaller than that of the bulk water (3.9 kcal mol$^{-1}$). This difference in $E^*$ values further supports our previous conclusion a few water molecules are hydrogen bonded in the plane of the cation and differ from the bulk water. This phenomenon can

 

be applicable to other hydrophobic solutes like amino acids, whose interactions with GdmCl leads to denaturation of protein.

## Conclusion

In the present study, the temperature-dependent, femtosecond resolved environmental dynamics in bulk water and in GdmCl solutions have been monitored. The activation energy of bound to free water interconversion has been estimated to be 3.6 kcal $mol^{-1}$. The increased solubility of C500 in water indicates preferential interaction of the probe with GdmCl. The results indicate that the reporter probe C500 is located in the solvation shell of the Gdm cation comprising of loosely bound water molecules. The residence of the probe in the solvation shell of the GdmCl cation have been confirmed through the increased microviscosity of the probe environment, compared to the bulk viscosity of solution. The study explores the hydrogen bonded structure and dynamics around the vicinity of a hydrophobic residue in GdmCl solutions, which might be similar to the environment around amino acids under denaturizing conditions.

## Acknowledgements

DB and PKV thank CSIR, India for fellowship. We thank DST for financial grant (SR/SO/BB-15/2007).

## References

1 F. H. Stillinger, *Science*, 1980, **209**, 451–457.
2 K. A. Sharp, B. Madan, E. Manas and J. M. Vanderkooi, *J. Chem. Phys.*, 2001, **114**, 1791–1796.
3 R. Mancicelli, A. Botti, M. A. Ricci and A. K. Soper, *Phys. Chem. Chem. Phys.*, 2007, **9**, 2959–2967.
4 R. Kumar, J. R. Schmidt and J. L. Skinner, *J. Chem. Phys.*, 2007, **126**, 204107.
5 A. W. Omta, M. F. Kropman, S. Woutersen and H. J. Bakker, *J. Chem. Phys.*, 2003, **119**, 12457.
6 R. Jimenez, G. R. Fleming, P. V. Kumar and M. Maroncelli, *Nature*, 1994, **369**, 471–473.
7 W. Jarzeba, G. Walker, A. E. Johnson, M. A. Kahlow and P. F. Barbara, *J. Phys. Chem.*, 1988, **92**, 7039–7041.
8 W. H. Cox and J. H. Wolfenden, *Proc. R. Soc. London, Ser. A*, 1934, **145**, 475–488.
9 H. S. Frank and F. Franks, *J. Chem. Phys.*, 1968, **48**, 4746.
10 R. D. Mountain and D. Thirumalai, *J. Phys. Chem. B*, 2004, **108**, 19711–19716.
11 E. G. Finer, F. Franks and M. J. Tait, *J. Am. Chem. Soc.*, 1972, **94**, 4424–4429.
12 B. Hribar, N. T. Southall, V. Vlachy and K. A. Dill, *J. Am. Chem. Soc.*, 2002, **124**, 12302–12311.
13 A. W. Omta, M. F. Kropman, S. Woutersen and H. J. Bakker, *Science*, 2003, **301**, 347–349.
14 D. Banerjee, S. S. Sinha and S. K. Pal, *J. Phys. Chem. B*, 2007, **111**, 14239–14243.
15 M. Kumbhakar, T. Goel, T. Mukherjee and H. Pal, *J. Phys. Chem. B*, 2004, **108**, 19246–19254.
16 M. L. Horng, J. A. Gardecki, A. Papazyan and M. Maroncelli, *J. Phys. Chem.*, 1995, **99**, 17311–17337.
17 S. Pal, S. Balasubramanian and B. Bagchi, *J. Phys. Chem. B*, 2003, **107**, 5194–5202.
18 R. K. Mitra, S. S. Sinha and S. K. Pal, *Langmuir*, 2008, **24**, 49–56.
19 S. K. Pal and A. H. Zewail, *Chem. Rev.*, 2004, **104**, 2099.
20 P. L. Moore Plummer, *THEOCHEM*, 1997, **417**, 35–47.
21 C. F. Chapman and M. Maroncelli, *J. Phys. Chem.*, 1991, **95**, 9095–9114.
22 Y. Nozaki and C. Tanford, *J. Biol. Chem.*, 1963, **238**, 4074–4081.
23 E. P. Kirby Hade and C. Tanford, *J. Am. Chem. Soc.*, 1967, **89**, 5034.
24 M. Bloemendal and G. Somsen, *J. Am. Chem. Soc.*, 1985, **107**, 3426.
25 M. Maroncelli, *J. Mol. Liq.*, 1993, **57**, 1–37.
26 V. Marcus, *Ion Solvation*, Wiley, New York, 1985.
27 B. Bagchi, *Chem. Rev.*, 2005, **105**, 3197–3219.
28 N. Nandi and B. Bagchi, *J. Phys. Chem. B*, 1997, **101**, 10954–10961.
29 E. Neria and A. Nitzan, *J. Chem. Phys.*, 1994, **100**, 3855–3868.
30 A. Chandra, *Chem. Phys. Lett.*, 1995, **244**, 314–320.
31 J. Peon, S. K. Pal and A. H. Zewail, *Proc. Natl. Acad. Sci. U. S. A.*, 2002, **99**, 10964–10969.
32 D. R. Lide, *CRC Handbook of Chemistry and Physics*, CRC Press Boca Raton, FL, 2005.
33 L. A. Philips, S. P. Webb and J. H. Clark, *J. Chem. Phys.*, 1985, **83**, 5810.
34 B. Kalman, N. Clarke and L. B. A. Johansson, *J. Phys. Chem.*, 1989, **93**, 4608–4615.
35 N. Ito, O. Kajimoto and K. Hara, *Chem. Phys. Lett.*, 2000, **318**, 118–124.
36 C. M. Hu and R. Zwanzig, *J. Chem. Phys.*, 1974, **60**, 4354–4357.
37 P. E. Mason, G. W. Neilson, C. E. Dempsey, A. C. Barnes and J. M. Cruickshank, *Proc. Natl. Acad. Sci. U. S. A.*, 2003, **100**, 4557.
38 S. K. Pal, J. Peon, B. Bagchi and A. H. Zewail, *J. Phys. Chem. B*, 2002, **106**, 12376–12395.
39 S. Sen, S. Mukhrerjee, A. Halder and K. Bhattacharya, *Chem. Phys. Lett.*, 2004, **385**, 357.
40 S. Balasubramanian, S. Pal and B. Bagchi, *Phys. Rev. Lett.*, 2002, **89**, 115505.
41 M. W. Feyereisen, D. Feller and D. A. Dixon, *J. Phys. Chem.*, 1996, **100**, 2993.
42 R. Zana, *J. Phys. Chem. B*, 1999, **103**, 9117–9125.